

Sudden warming epochs during 42 to 28 ky BP in the Himalayan region from stable isotope record of sediment from a relict lake in Goting, Garhwal, North India

Prosenjit Ghosh^{#,†} and S. K. Bhattacharya*

[#]Max-Planck-Institute for Biogeochemistry, Winzerlaer Str. 10, 07745 Jena, Germany

*Physical Research Laboratory, Navarangpura, Ahmedabad 380 009, India

¹⁸O/¹⁶O variations of the precipitation recorded in carbonate sediments of a high-altitude Himalayan lake have been investigated by analysing samples from a varve deposit in Goting, Garhwal Himalaya. ¹⁴C ages of four samples from different depths suggest that the sedimentation in the lake started ~ 42 ky BP and continued till ~ 28 ky BP. Fluctuations in $d^{18}\text{O}$ values are interpreted in terms of water-source variations. A trend showing the enrichment of $d^{18}\text{O}$ values between 32 and 28 ka indicates slow cooling as one approaches the Last Glacial Maximum (LGM). There are six strong $d^{18}\text{O}$ excursions (depleted ratios) coinciding with low ¹³C values at around 40.2, 38.2, 36.2, 34.2, 32.8 and 29.4 ky BP, denoting enhancement of the southwest monsoon. In addition, three positive shifts at around 40.7, 37.2 and 35.2 ky BP were observed, which indicate weakening of the southwest monsoon. Fourier analysis of the $d^{18}\text{O}$ time series shows a significant ~ 740 year periodicity, similar to that reported in the Arabian Sea and South China Sea.

THE history of global climate change during the last glacial cycle is faithfully recorded in two repositories, i.e. deep-sea sediments and ice sheets¹. From these records it has been established that the slow cooling and warming phases in this cycle were punctuated by several relatively short-term events signifying instabilities in the climate system. However, such variation in the continental climate is relatively less clear because of absence of suitable archives preserving continuous record. In this context, palaeo-lakes have special importance. Lakes are smaller water bodies compared to oceans and ice sheets, and are, therefore, sensitive to even small climatic fluctuations; may contain records of sudden environmental changes in their sediments. However, continuous sedimentary sequences from lakes are rare, especially from the tropical region. Recent discovery of a varve sediment deposit in Goting palaeo-lake, Garhwal Himalaya by Pant *et al.*² has

led to the possibility of deriving past climatic information from a study of the layers of the deposit. Geological evidences indicate that this deposit, presently exposed as a standing column, formed in a lake with fluctuating margins. It is believed that the lake originated as a result of impounding of the river Dhauli-Ganga by landslides (Figure 1) and drained out later when the breach got removed due to another phase of tectonism. Based on morphological features and ¹⁴C dates, Pant *et al.*² argued in favour of a continuous sedimentation during the life of the Goting lake (from about 42 to 28 ky BP). Magnetic susceptibility studies along its length showed marked enhancement of susceptibility at about 36.5 ka (ref. 2). Increase in the magnetic susceptibility coincided with increase in the occurrence of limonitic bands comprising hematite and goethite minerals. Since formation of these

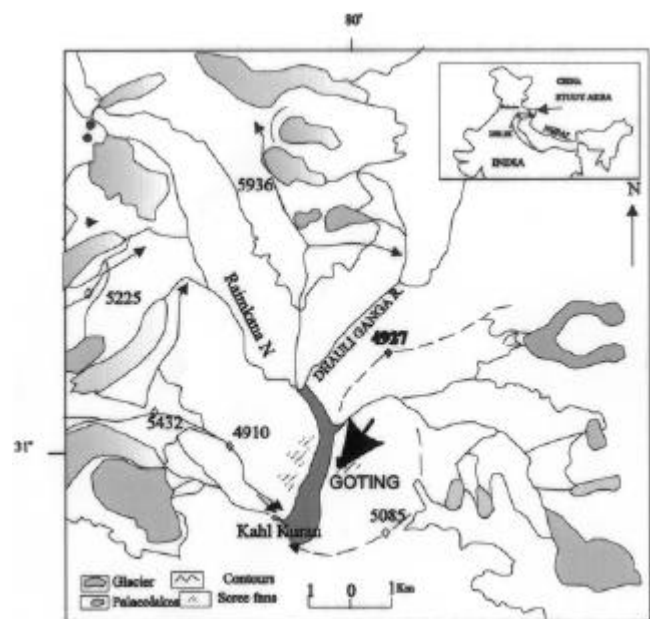


Figure 1. Location of the Goting relict lake deposit in Garhwal Himalaya. The glaciers at higher reaches (> 1000 ft w.r.t. the Goting basin) feeding the stream Dhauli-Ganga and sampling site (denoted by a box) are also shown.

[†]For correspondence. (e-mail: pghosh@bgc-jena.mpg.de)

minerals is favoured in warmer conditions, the 36.5 ka event was interpreted² as a period of climatic amelioration.

A major component of the Goting sediments consists of marly carbonates and offers the possibility of carbon and oxygen isotope analysis in the annual layers to infer about the water source and its variation. As in the other Himalayan rivers from this region, the river Dhaulī–Ganga receives its water from monsoonal rainfall, winter snowfall and melting of glacier. These sources of water are expected to have different stable (O, H) isotopic composition and, therefore, any variation in their relative supply would lead to isotopic variation in the Goting lake and in the contemporary authigenic carbonate phase. Our study was motivated to decipher such variation in the geological history of the lake, with possible connection to climate change in this region.

Materials and methods

A 15 m thick sedimentary pile comprising alternate bands of coarse and fine marly sediments (Figure 2) from a cliff face was chosen for sampling. Samples were collected starting from ground level up to a height of 12 m (Table 1). Adequate precaution was taken while sampling to avoid recent contamination and cross-contamination between two neighbouring samples. About 200 samples were collected from different layers (fine- and coarse-grained). Thin-section study of some chips showed that the samples are composed of detrital (quartz and feldspar) material with micritic carbonate as cementing matrix having grains less than 100 micron in size. The fine-grained nature of the matrix, the layered structure and absence of features suggesting re-precipitation of carbonates indicate that they are primary precipitates and have not suffered any alteration subsequent to precipitation. An additional

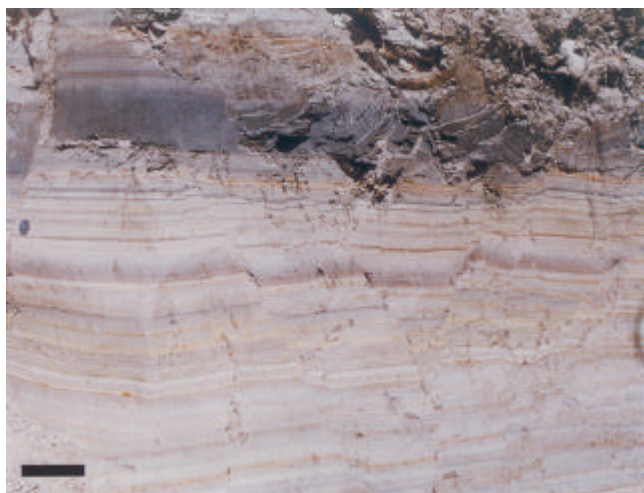


Figure 2. Exposure of rhythmite showing alternate laminations of fine (dark colour) and coarse (light colour) material at Goting (bar 20 cm in length).

confirmation for this is provided by the nature of the isotopic data itself, displaying large differences in adjacent layers. Ages of six samples (bulk organic phase) at different depths were determined earlier using radiocarbon technique². Oxygen and carbon isotopic composition of the carbonate cement was measured after crushing the sample chips to fine powder (~200 mesh) and reacting with 100% phosphoric acid at 25°C for 12 h. The carbon dioxide produced by the reaction was cleaned and purified cryogenically and analysed in a VG Micromass 903 mass-spectrometer. Water samples, collected from snowmelt, rainfall and river were also analysed following the procedure of CO₂ equilibration at 25°C (ref. 3). A number of samples were re-analysed to check the sample heterogeneity. The isotopic ratios of carbon and oxygen are presented in the usual *d* notation in units of per mil (‰) w.r.t. V-PDB and are reproducible within 0.1‰ at 1 *s* level. The oxygen isotopic ratios of the water samples are expressed w.r.t. V-SMOW.

Chronology of the Goting sediments

Pant *et al.*² determined ¹⁴C ages for six samples from the same Goting section (Table 2). These ages were obtained from the organic fraction of the sediments, but were not corrected for variation in radiocarbon production function in the past. This needs to be done in order to make reliable inter-comparison with other proxy climate data. A calibration curve based on tree ring, varve counting and coral dating is available for the period 0–24 ky BP (ref. 4). Beyond 24 ky BP, a calibration has been proposed by Bard *et al.*⁵ based on U–Th dates and ¹⁴C ages of coral samples. According to this, the true age is 1.168 times the measured ¹⁴C age. This factor is used here for estimating the correct ages of the six Goting samples (Table 2). Out of the six ages, two are found to deviate from a linear trend probably due to contamination by younger carbon². Four corrected ages were plotted against the sample depths and a linear regression line was drawn. An average annual sedimentation rate of 1.2 mm/yr is obtained from the slope of this line. This estimate is higher than the earlier estimate of 0.7 mm/yr obtained by Pant *et al.*² using all the six uncalibrated ages.

Results

The oxygen and carbon isotopic ratios of the carbonate cements are plotted in Figure 3 *a* and *b* along with the estimated ages of the samples. The samples are not strictly equally spaced and the time difference between two adjacent samples ranges from 60 to 100 yrs. The average *d*¹⁸O value based on 193 samples (rejecting the values of seven samples with outlier values) is –14‰ with a 1 *s* range of ±2.3‰. The corresponding mean *d*¹³C value is –0.8‰, with a 1 *s* range of ±1.0‰. The oxygen isotopic

Table 1.

GS sample	Depth (cm)	Cal age (BP year)	$d^{13}\text{C}$ (PDB)	$d^{18}\text{C}$ (PDB)
1	5	42546	-1,6	-15,0
2	12	42460	0,0	-11,2
3	15	42423	-1,2	-15,1
4	23	42325	-2,1	-17,0
5	32	42315	-2,9	-17,3
6	43	42081	-1,4	-13,9
7	58	41897	-1,8	-16,0
8	68	41775	-1,0	-14,5
9a	79	41640	-1,1	-15,5
9b	74	41701	-1,0	-13,7
10	86	41554	-0,2	-11,9
11	93	41469	-2,2	-15,8
12	98	41407	-1,6	-14,2
13	103	41346	-1,5	-15,6
14	108	41285	-1,6	-12,3
15	112	41236	-1,8	-16,2
16	115	41199	-0,8	-12,6
17	117	41175	-1,0	-14,8
18	123	41101	-0,4	-10,9
19	128	41040	-0,0	-12,4
20	132	40991	-0,8	-15,3
21	137	40930	0,3	-11,6
22	143	40857	-0,4	-12,5
23	150	40771	-2,4	-19,1
24	158	40673	-1,8	-17,1
25	166	40575	-1,0	-14,4
26	174	40477	-1,3	-15,4
27	186	40330	-0,9	-13,6
29	204	40110	-2,3	-11,6
30	214	39988	-0,3	-13,3
31	222	39890	-2,1	-19,2
32	236	39718	-1,1	-13,9
33	246	39596	-0,5	-12,4
34	260	39425	-1,7	-18,4
35	278	39204	-1,0	-14,2
36	284	39139	-1,9	-16,8
37	291	39045	-1,5	-15,5
38	299	38947	-0,3	-12,6
39	307	38849	-0,3	-13,0
40	316	38739	-0,0	-12,6
41	326	38617	-1,1	-14,5
42	336	38494	-0,3	-12,0
43	347	38360	-2,3	-14,4
44	356	38250	-2,2	-17,6
45	365	38139	-1,6	-16,6
46	375	38017	-2,9	-12,0
47	385	37895	-2,6	-15,5
48	395	37772	-2,8	-18,5
49	405	37650	-1,9	-17,3
50	415	37527	-0,2	-12,0
51	425	37405	-0,1	-12,4
52	431	37332	-0,5	-12,0
53	436	37270	-0,4	-13,2
54	445	37160	-1,2	-14,3
55	455	37038	-0,8	-13,1
56	461	36964	0,6	-10,1
57	466	36903	-0,2	-11,8
58	471	36842	-2,8	-19,6
59	474	36805	-0,9	-13,8
60	478	36756	-1,5	-13,4
61	482	36707	-1,4	-16,5
62	486	36658	-0,9	-13,7
63	491	36597	-0,6	-13,4
64	496	36536	-0,3	-13,5
65	502	36463	-1,4	-15,8
66	507	36401	0,0	-11,2
68	515	36303	-0,4	-12,5
69	519	36254	-2,1	-19,0
70	526	36169	-2,2	-19,1

(Table 1. Contd.)

GS sample	Depth (cm)	Cal age (BP year)	$d^{13}\text{C}$ (PDB)	$d^{18}\text{C}$ (PDB)
71	532	36095	-1,2	-15,1
72	539	36010	-2,1	-16,4
73	545	35936	-0,2	-10,2
74	552	35851	-0,3	-13,7
75	565	35691	-0,1	-11,0
76	575	35569	-2,1	-16,9
77	582	35483	-0,6	-12,6
78	588	35410	-0,4	-12,1
79	592	35361	-0,9	-13,9
80	597	35300	0,4	-11,0
81	601	35259	-2,0	-16,8
82	603	35226	-0,1	-12,2
83	607	35177	-0,5	-12,3
84	612	35116	0,2	-11,5
85	617	35055	-1,0	-14,3
86	621	35006	-0,8	-12,4
87	624	34969	-0,9	-13,9
88	629	34908	0,8	-10,5
89	633	34859	-3,1	-18,4
90	638	34798	-0,3	-9,0
91	642	34749	-0,3	-13,8
92	647	34688	-0,2	-12,9
93	652	34627	-2,4	-17,9
94	658	34553	-1,2	-14,9
96	667	34443	-0,7	-13,8
97	672	34382	-1,4	-13,8
98	678	34308	-2,2	-19,9
99	686	34210	-0,7	-13,8
100	690	34161	-0,4	-12,0
101	697	34076	-2,5	-20,2
102	706	33966	-0,1	-13,9
103	713	33880	-1,1	-15,9
104	718	33819	0,6	-11,5
105	723	33757	-1,6	-18,0
106	727	33709	0,1	-12,6
107	731	33660	0,0	-13,6
108	734	33623	0,1	-12,8
110	741	33537	0,4	-12,2
111	746	33476	-1,8	-17,1
112	752	33403	0,3	-11,7
113	757	33341	0,2	-13,4
114	762	33280	0,0	-12,0
115	766	33231	0,7	-14,0
116	771	33170	0,5	-12,0
120	788	32962	-0,8	-14,2
121	792	32913	-2,5	-16,7
122	796	32864	-1,8	-14,5
123	799	32827	-4,4	-18,5
124	802	32791	-2,7	-17,3
125	806	32742	-3,4	-18,0
127	816	32619	-1,7	-16,5
128	820	32570	-1,1	-11,4
129	827	32485	-0,1	-12,4
130	832	32423	-0,2	-12,9
131	837	32362	-1,5	-15,0
132	840	32325	-0,2	-12,9
133	844	32276	-1,5	-16,2
134	848	32227	-1,2	-12,7
135	852	32179	-1,1	-13,0
136	855	32142	3,1	-9,4
137	859	32093	0,3	-11,5
138	863	32044	-0,9	-14,2
139	868	31983	-0,2	-13,2
140	871	31946	-0,5	-11,7
141	874	31909	-0,3	-12,4
142	879	31848	-0,9	-14,0
143	883	31799	-1,8	-14,8
144	888	31738	-0,6	-13,6
145	892	31689	-1,0	-15,6

(Table 1. Contd.)

(Table 1. *Contd.*)

GS sample	Depth (cm)	Cal age (BP year)	$d^{13}\text{C}$ (PDB)	$d^{18}\text{O}$ (PDB)
146	896	31640	0,4	- 11,0
147	901	31579	- 0,1	- 13,8
148	907	31505	- 1,1	- 15,6
149	914	31420	- 0,5	- 13,4
150	921	31334	- 1,5	- 15,7
151	928	31248	- 0,6	- 12,8
152	935	31163	0,2	- 12,1
153	939	31114	- 0,7	- 13,8
154	944	31052	- 1,1	- 14,4
155	951	30967	- 0,9	- 15,6
156	958	30881	- 0,3	- 11,7
157	963	30820	0,6	- 11,0
158	968	30759	- 0,2	- 14,0
159	973	30697	- 0,2	- 13,2
160	977	30649	- 1,7	- 16,8
161	981	30600	- 0,7	- 15,0
162	985	30551	- 0,4	- 14,0
163	988	30514	1,1	- 10,2
164	992	30465	0,0	- 13,1
165	997	30404	- 0,8	- 13,9
166	1002	30343	- 1,2	- 16,4
167	1007	30281	0,7	- 11,0
168	1012	30220	0,4	- 12,2
169	1017	30159	- 1,6	- 17,7
170	1020	30122	0,2	- 12,0
171	1027	30037	- 0,7	- 14,0
172	1035	29939	0,4	- 11,1
173	1042	29853	1,5	- 9,5
174	1046	29804	- 0,6	- 13,9
175	1051	29743	- 0,2	- 13,8
176	1056	29682	- 0,7	- 11,7
177	1061	29620	- 1,4	- 16,2
178	1065	29571	- 0,4	- 14,7
179	1069	29522	- 1,5	- 16,2
180	1074	29461	- 0,4	- 14,1
181	1080	29388	- 0,8	- 14,9
182	1087	29302	- 0,8	- 15,0
183	1094	29216	0,0	- 13,2
184	1102	29119	- 0,5	- 14,2
185	1108	29045	0,2	- 12,7
186	1112	28996	1,0	- 10,9
187	1126	28825	- 1,3	- 15,8
188	1134	28727	0,5	- 11,0
189	1141	28641	- 0,9	- 16,1
190	1147	28562	0,8	- 11,9
191	1152	28507	- 1,0	- 12,7
192	1156	28458	0,5	- 12,0
193	1165	28347	- 1,1	- 12,0
194	1173	28249	- 1,5	- 17,0
195	1178	28188	- 0,9	- 15,7
196	1185	28103	- 0,7	- 14,0
197	1193	28005	- 0,4	- 14,6
198	1203	27882	0,4	- 12,1
199	1210	27797	- 0,9	- 16,4
200	1218	27699	0,0	- 13,3

composition of various possible sources of water in this region was also measured for comparison with past values. Samples of fresh snow, river water and glacier melt-water close to the Goting section have $d^{18}\text{O}$ values of - 13.5, - 13.0, and - 20.3‰ (mean of two samples), respectively. The $d^{13}\text{C}$ values of the cements vary typically from - 3 to 1‰ (Figure 3 b). Variation in the case of carbon is smaller compared to that of oxygen. The depth variation of both $d^{18}\text{O}$ and $d^{13}\text{C}$ is characterized

Table 2.

Sample	Depth (cm)	Age (Pant <i>et al.</i> ²)	Calibrated age (Bard <i>et al.</i> ³)
9a	79	36,000 ± 2880	42,048 ± 2880
55	455	38,410 ± 4130	44,863 ± 4130
9	519	32,760 ± 2370	38,264 ± 2370
135	852	20,420 ± 1710	23,851 ± 1710
169	1017	26,610 ± 2370	31,080 ± 2370
197	1193	24,230 ± 1550	28,301 ± 1550

by sharp oscillations numbering about 40 over the whole section. While there is a large variation in amplitude and duration of the oscillations, the average amplitude for $d^{18}\text{O}$ oscillation is about 7‰ and that for $d^{13}\text{C}$ is about 2‰. The average duration of oscillation is about 200 yrs.

Discussion

The oxygen and carbon isotopic compositions of the carbonate phase in lake sediments are determined by composition of these isotopes in water and the temperature of precipitation. The sedimentary sequence of Goting represents a continental record corresponding to the glacial stage 3 (Oxygen Isotope Stage 3 is 60,000–25,000 [CAL] years ago) of the marine oxygen isotope record in the last glacial cycle. During this stage, carbonates were precipitated from the lake water along with the lake sediments (composed of detritals). These carbonates act as a firm binding material and allow preservation of dark and light lamination in the sedimentary column. Dark bands represent cold, non-turbulent conditions when the lake water constituents (bed load) are mainly fine particles, like clays along with organics. In contrast, light bands are mainly composed of slightly coarser particles free of organic matter, reflecting turbulent, high-discharge condition. The same is reflected in the isotopic composition. The proportion of carbonate in the dark bands is smaller (5–10%) compared to the light band (20–25%). We next describe the significance of the isotopic variations of carbonate in terms of climatic changes in this region.

Mean oxygen isotopic composition of lake water

It is important to note that despite the large range in $d^{18}\text{O}$ values (- 9 to - 22‰) majority of the values fall in a cluster and follow a Gaussian pattern with minor spread (~ 2.3‰). This allows calculation of a representative mean (- 14‰) and also to deduce a mean value for the pore-water composition which can be used to estimate the average composition of the precipitation during that period. To estimate the composition of water from the $d^{18}\text{O}$ value of the carbonate, the temperature of precipitation of calcite at the lake bottom needs to be assessed. The Goting basin is located in the Himalayan region

where mean annual temperature is 13.5°C (from meteorological data (ref. 6) at Mukteswar, Kumaun). We assume this value as the mean temperature of water in the Goting lake and derive the fractionation factor α between carbonate and water from the Friedman and O'Neil⁷ equation ($10^3 \ln \alpha = 2.78 \cdot 10^6 / T^2 - 2.89$) as $\alpha = 1.0314$. α is related to $d^{18}\text{O}$ of calcite by: $\alpha = (d^{18}\text{O}_{\text{calcite}} + 1000) / (d^{18}\text{O}_{\text{water}} + 1000)$. Using the mean $d^{18}\text{O}$ value of Goting carbonate (-14% w.r.t. V-PDB or 16.4% w.r.t. V-SMOW), the estimated isotopic composition of pore-water ($d^{18}\text{O}_{\text{water}}$) is $-14.6 \pm 2.3\%$ w.r.t. V-SMOW.

The estimated composition of the lake water differs only slightly (0.9 and 1.6‰) from present-day snow and river water composition, whereas the difference is large for glacial melt-water (5.7‰). This suggests that the major source of water in the lake was rain or snow. The glaciers occurring at higher reaches (> 1000 ft above the Goting basin) receive snowfall with depleted isotopic composition because of their altitude. Since the Goting lake formed in a cooler period (Glacial Stage 3) the contribution from glacier melt was probably not significant.

Isotopic oscillations

The isotopic depth profile contains approximately 40 oscillations with extreme values of $d^{18}\text{O}$ varying from -9 to -21% . The alternate dark and light bands, denoting material deposited during cold and warm intervals caused such oscillations. This was validated by analysis of a few selected light bands showing depleted values compared to the dark bands. These oscillations took place typically over timescale of a few hundred years. To explain such large amplitude (about 7‰) oscillations, one needs to invoke either a change in temperature, amount of rainfall and enhanced supply of glacial melt water. Interestingly, in a region dominated by monsoon, all these factors are positively correlated while delivering the final isotopic composition in the water or resultant carbonate. An increase in land temperature tends to bring more rainfall and also increase the glacial melt-water supply. They also work in tandem in changing the carbonate isotopic ratio. For example, increase in temperature, glacial melt-water and rainfall all have the effect of depleting the heavy isotope, the temperature acting through the fractionation factor and the rainfall through the amount effect. Nevertheless, if we ascribe 7‰ variation solely to a temperature change, the estimated change in regional air temperature would be unacceptably large (about 28°C using $0.25\%/^{\circ}\text{C}$ as the temperature coefficient of fractionation between precipitating calcite and water medium). However, a small temperature effect of 2–3‰ (for change in temperature of ~ 8 – 12°C based on CLIMAP estimates⁸) cannot be ruled out. The rest of the depletion is, therefore, associated with change in water composition which, in turn, is due to change in amount of rainfall or greater supply of gla-

cial melt-water. IAEA data on rainfall and isotopic composition of mean monthly precipitation from a station in New Delhi yield an estimate of 0.34‰ decrease in $d^{18}\text{O}$ for 10 mm increase in mean monthly rainfall. If we assume this value as the representative coefficient for monsoonal rainfall, the amplitude of $d^{18}\text{O}$ variation (7‰) would give an estimate of 200 mm change in mean monthly rainfall. However, it is difficult to estimate the exact contribution of the above factors based on oxygen isotopic composition of carbonates. A comparative study was done by Thompson *et al.*⁹, who observed oscillations of similar magnitude in an ice core record from the Tibetan Plateau (Guliya) and interpreted them in terms of variations in the strength of the southwest monsoon.

Periodicity of small oscillations

Power spectrum analysis¹⁰ of $d^{18}\text{O}$ values from the Goting section reveals the presence of periodicity of ~ 275 , ~ 300 , ~ 465 , ~ 530 , ~ 740 yrs (Figure 3 c), with strongest power in the 740 ± 20 yr period. Recently, two isotopic studies based on planktonic foraminifera from the Arabian Sea sediments¹¹ and South China Sea sediments¹² have shown the presence of periodicities of 700 and 775 yrs comparable to the present 740 yr cycle.

Source of dissolved inorganic carbon in the lake

The carbon isotopic composition of the Goting carbonates is determined by contribution from two sources: CO_2 dissolved from the soil zone and dissolution of old marine carbonates (Tethys Himalayan sediments) in the river catchment. Production of CO_2 in the soil zone is mainly from decomposition of vegetative matters with average $d^{13}\text{C}$ values of -27 and -12.5% for C_3 and C_4 type plants, respectively¹³. Earlier studies on the carbon isotopic composition of organic matter in the Pleistocene sediments from Karewa region, Kashmir (~ 300 km northwest of Goting) showed that this region was dominated by C_4 type vegetation¹⁴. Since the soil CO_2 generated by plants is about 4.5‰ heavier than the plant biomass, the dissolved CO_2 would be characterized by $d^{13}\text{C}$ value of -8% (ref. 13). In contrast, dissolved bicarbonates derived from dissolution of old marine carbonates have $d^{13}\text{C}$ values between -2 and 1% (ref. 15). The mean $d^{13}\text{C}$ of -0.8% for the Goting carbonate is consistent with its derivation dominantly from Himalayan carbonates. The negative excursions would then correspond to occasional increase in the soil-derived component.

The carbon and oxygen isotopic ratios of the Goting carbonates are strongly correlated (Figure 4) as often found in sediments of a closed basin¹⁶. The positive correlation (correlation coefficient of 0.8) indicates a common causal origin in their variations. For example, during warm

periods (extended summer) this area is expected to receive high rainfall (enhanced summer monsoon with lower $d^{18}\text{O}$ in rains) which would allow enhanced growth and decay of vegetative matter. As a result, there would be larger contribution of CO_2 from the soil zone to the aqueous medium, leading to depleted isotopic values of carbon. In contrast, during the low rainfall season, the biogenic source would be less important and the dominant contribution of carbon would be from marine carbonates occurring in the river channel. Such a scenario would lead to covariation of $d^{18}\text{O}$ and $d^{13}\text{C}$ values in the carbonate.

Long term climatic change between 28 to 42 ky BP

As mentioned before the sampling resolution for the present study varied between 60 and 100 yrs and large-amplitude oscillations of $d^{18}\text{O}$ are observed over time-scales of a few centuries. The Goting record can be compared with a climatic record based on $^{18}\text{O}/^{16}\text{O}$ ratios in an ice core at Guliya on the Tibetan plateau⁹. However, since the Guliya record is of lower resolution, to compare the two records, the moving average of $d^{18}\text{O}$ values of successive 10 points (representing about 500 yrs) in the Goting record is calculated and a curve is drawn through these average values plotted against the average age (Figure 5 *a* and *b*). The resultant curve filters out high-frequency signals and brings out the longer term variations in $d^{18}\text{O}$ and $d^{13}\text{C}$ between 42 and 28 ky BP. These two curves

show a systematic increasing trend (shown by a line in Figure 4 *a* and *b*), indicating about 1‰ increase in both $d^{18}\text{O}$ and $d^{13}\text{C}$ while going from 42 to 28 ky BP. This increase is consistent with the expectation, since while going from 42 to 28 ky BP one is approaching the Last Glacial Maximum (LGM) (~ 20 ky BP) and, therefore, towards a colder regime with consequent increase in $d^{18}\text{O}$ of precipitating carbonate in colder lake water. Figure 5 *a* also shows six epochs (around 40.2, 38.2, 36.2, 34.2, 32.7 and 29.4 ka) when $d^{18}\text{O}$ of carbonates decreased rapidly from the average trend. Each epoch is shown by an arrow in Figure 5 *a* and marks a minima in the $d^{18}\text{O}$ curve. Hatched regions in Figure 5 *a* demarcate the zones with lower than normal values (estimated from the trend line). These excursions are characterized by nearly symmetrical decrease and recovery of $d^{18}\text{O}$ values in all the epochs. These epochs probably represent short-duration events of increased rainfall caused by regional warming, with warmer intervals ranging from 1000 to 2000 yrs. It is of interest to compare these events with seven Dansgaard–Oeschger warming events during this time interval recorded in Greenland ice core, which occurred around 29, 30.2, 32, 34.8, 36.9, 37.8, and 39.5 ky BP (ref. 17). Adjusting for slight mismatch in timing, the number of events matches closely with the number obtained here and could have a common cause. As expected from correlation between oxygen and carbon isotope ratios, $d^{13}\text{C}$ values also become more negative during these intervals (Figure 5 *b*), signifying increased contribution of bio-

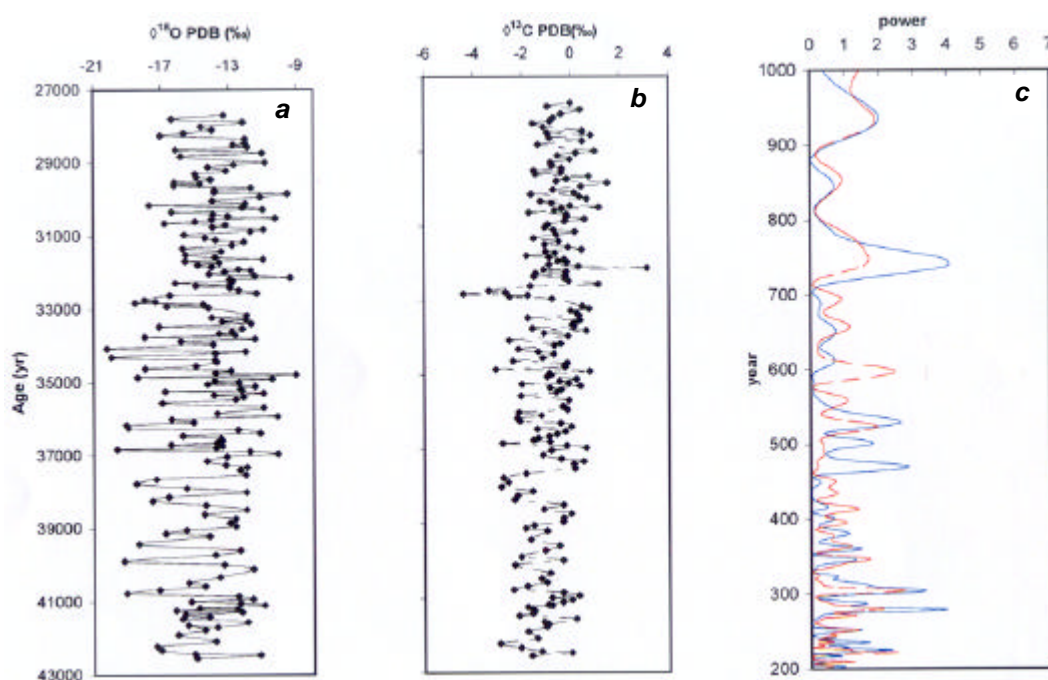


Figure 3. *a*, Variation of oxygen isotope ratio in the carbonate cement (w.r.t. PDB); *b*, Variation of carbon isotope in the carbonate cement (w.r.t. PDB). $d^{18}\text{O}$ values show large magnitude of variation compared to $d^{13}\text{C}$; *c*, Power spectrum of the measured $d^{18}\text{O}$ and $d^{13}\text{C}$. Note six significant periodicities of which 740 year period has highest power.

genic CO₂ through increased rainfall, and marking intervals of major climatic amelioration. The magnitude of the excursions increases from older to younger epochs (from ~ 1 to 2‰), probably indicating increasing instability and associated variability as one approaches the LGM.

In Figure 5 *c*, existing oxygen isotope record between 42 and 28 ky BP from Guliya ice core is plotted for comparison. Broadly, the two patterns are not similar.

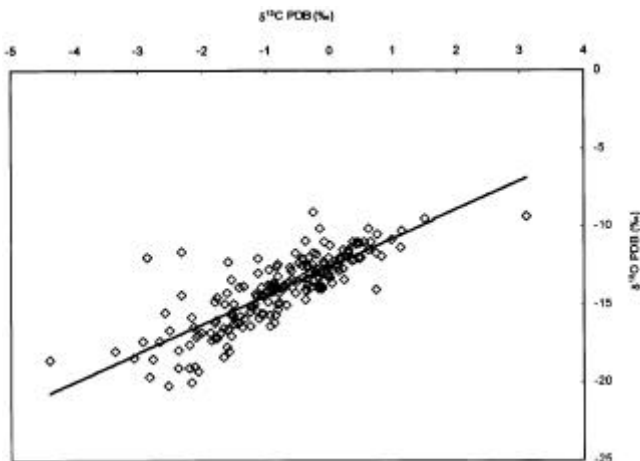


Figure 4. Covariation plot of oxygen and carbon isotopic ratios in micritic calcite cements of varve. Strong positive covariance ($r = 0.82$) is noted.

However, in the Guliya record the period between 42 to 34 ky BP contains three major epochs (40.7, 37.2 and 35.2 ka), when there is clustering of data points with depleted $d^{18}O$ values (encircled in Figure 5 *c*); and these have corresponding changes in the Goting record. These depletions probably denote periods when strong northeasterly wind brought moisture from continental sources or oceanic sources from long distances⁹. If these periods indicate short spells of intense cool intervals, we expect enriched $d^{18}O$ phases in corresponding periods in the Goting record, as indeed is the case (indicated by P1, P2 and P3 in Figure 5 *a*). However, limitation of resolution and time assignment in the Guliya core⁹ does not allow finer comparison.

The period between 34 to 28 ky BP shows systematic drop in $d^{18}O$ values in the ice core samples (Figure 5 *c*). Such a drop probably indicates strengthening of NE monsoon carrying depleted moisture from long distances as one is approaching the LGM. The corresponding increase in $d^{18}O$ of the carbonates during this interval indicates a drop in temperature and is consistent with the above hypothesis. During the above period, two major epochs (34.2 and 32.8 ka) of negative $d^{18}O$ are observed in the Goting record. These epochs are absent in the Guliya record. We propose that these epochs indicate periods with abrupt increase in precipitation caused by enhanced SW monsoon. Such changes in precipitation would show

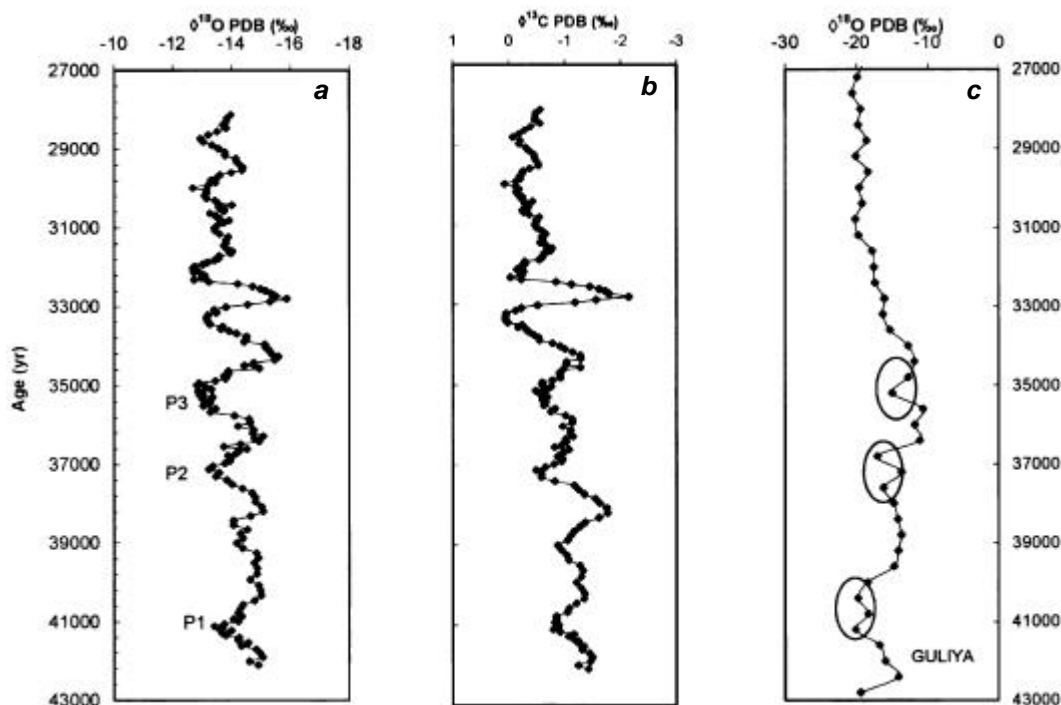


Figure 5. *a*, Ten-points moving average curve based on 10 sequential oxygen isotope values of carbonate cements. Note overall trend of increase in $d^{18}O$ in the younger samples as one approaches the LGM; *b*, Ten-points moving average curve based on 10 sequential carbon isotope values in the carbonate cements; *c*, Proxy data from Guliya ice core record of Tibetan plateau (L. G. Thompson, pers. commun.) plotted for comparison. Note epochs of low $d^{18}O$ values denoted by P1, P2 and P3 signifying cold events in the contemporary lake record.

up in the Goting record, but not in Guliya which falls in a region controlled more by NE monsoon.

Conclusions

Section of a varved, sedimentary column has been recently discovered² from a relict lake in Goting locality, Garhwal Himalaya, which contains marly carbonate (calcite) grains. These sediments were deposited during the interval 42 to 28 ky BP based on ¹⁴C ages. Oxygen and carbon isotope ratios in the calcite were measured to understand the variation in the water composition of the lake and infer the causes of variation in terms of changes in climate during the stage 3 of the last glacial cycle. There is systematic increase in both the isotope ratios, indicating gradual cooling with time. The time variation of the isotope ratios shows short-term oscillations with periods of a few hundred years similar to the Dansgaard-Oeschger events in Greenland ice core records. Power spectrum analysis shows that a periodicity of 740 ± 20 yr has the strongest power. This is consistent with periodicity of 700 and 775 yrs based on foraminiferal isotope record from the Arabian Sea and South China Sea, respectively. The record also shows six epochs (40.2, 38.2, 36.2, 34.2, 32.7 and 29.4 ky BP) where sharp, negative shifts in $d^{18}O$ and $d^{13}C$ of carbonates were observed. These epochs indicate intervals of enhanced southwest monsoon associated with increased rainfall. In addition, there are three epochs (41.5, 37 and 35 ky BP) of short positive shifts in $d^{18}O$ values indicating weakening of southwest monsoon, which coincides with enhancement of northeast monsoon in this region based on an ice core record from Guliya.

1. *Palaeoclimates and Palaeowaters: A Collection of Environmental Isotopes Studies*, Panel Proceedings Series, IAEA, Vienna, 1983, p. 207.
2. Pant, R. K., Juyal, N., Rautela, P., Yadav, M. G. and Sangode, S. J., Climate instability during last glacial stage: Evidence from varve deposits at Goting, district Chamoli, Garhwal Himalay, India, *Curr. Sci.*, 1998, **75**, 850–855.
3. Bhattacharya, S. K., Gupta, S. K. and Krishnamurthy, R. V., Oxygen and hydrogen isotopic ratios in groundwaters and river waters from India, *Proc. Indian Acad. Sci. (Earth Planet Sci.)*, 1985, **94**, 283–295.
4. Stuiver, M. *et al.*, INTCAL 98 Radiocarbon age calibration, 24000–0 cal BP, *Radiocarbon*, 1998, **40**, 1041–1083.

5. Bard, E., Arnold, M., Hamelin, B., Laborde, N. T. and Cabioch, G., Radiocarbon calibration by means of mass spectrometric ²³⁰Th/²³⁴U and ¹⁴C ages of corals: An update database including samples from Barbados, Mururoa and Tahiti, *Radiocarbon*, 1998, **40**, 1085–1092.
6. India Meteorological Department Climatological Tables of Observatories in India, 1931–1960, p. 457.
7. Friedman, I. and O'Neil, J. R., Compilation of stable isotope fractionation factors of geochemical interest. in *Data of Geochemistry* (ed. Fleischer, M.), US Geological Survey, Professional Paper 440-K, 1977, 6th edn, pp. 1–12.
8. CLIMAP, Seasonal reconstruction of the earth's surface at the Last Glacial Maximum. Geological Society of America, Map Chart Series MC-36, Boulder, Colorado, 1981.
9. Thompson, L. G. *et al.*, Tropical Climate Instability: The Last Glacial Cycle from a Qinghai–Tibetan Ice Core, *Science*, 1997, **276**, 1821–1825.
10. Press, W. H., Teukolsky, S. A., Vetterling, W. T. and Flannery, B. P., *Numerical Recipes in FORTRAN*, Cambridge University Press, Cambridge, 1992, p. 569.
11. Sarkar, A., Ramesh, R., Somayajulu, B. L. K., Agnihotri, R., Jull, A. J. T. and Burr, G. S., High resolution Holocene monsoon record from the eastern Arabian Sea, *Earth Planet. Sci. Lett.*, 2000, **177**, 209–218.
12. Wang, L. *et al.*, East Asian monsoon climate during the Late Pleistocene: High resolution sediment records from the south China Sea, *Mar. Geol.*, 1999, **156**, 245–284.
13. Vogel, J. C., Variability of carbon isotope fractionation during photosynthesis. in *Stable Isotopes and Plant Carbon Water Relations* (eds Ehleringer, J. R., Hall, A. E. and Farquhar, G. D.), Academic Press, San Diego, CA, 1993, pp. 29–38.
14. Krishnamurthy, R. V., Niro, M. D. De and Pant, R. K., Isotopic evidence for Pleistocene climate changes in India, *Nature*, 1982, **298**, 640–641.
15. Valero-Garces, B. L., Delgado-Huertas, A., Ratto, N. and Navas, A., Large ¹³C enrichment in primary carbonates from Andean Altiplano lakes, North West Argentina, *Earth Planet. Sci. Lett.*, 1999, **171**, 253–266.
16. Talbot, M. R., A review of the palaeohydrological interpretation of carbon and oxygen isotopic ratios in primary lacustrine carbonates, *Chem. Geol.*, 1990, **80**, 261–279.
17. Bond, G. C. and Lotti, R., Iceberg discharges into the North Atlantic on millennial time scales during the last glaciation, *Science*, 1995, **267**, 1005–1009.

ACKNOWLEDGEMENTS. We thank the team members of the expedition for painstakingly collecting samples from the rugged terrain bordering Tibet in Central Himalayas. We also thank Mr M. Yadava for providing us the calibrated ages of the samples and Mr Soumen Mondal for time series analysis. This work is a contribution to the project on Quaternary glaciation undertaken with financial support from the Department of Science and Technology, Govt. of India.

Received 25 October 2002; revised accepted 1 March 2003